J. Biochem. **137**, 255–263 (2005)
DOI: 10.1093/jb/mvi039

NMR Study on the Major Mite Allergen Der f 2: Its Refined Tertiary Structure, Epitopes for Monoclonal Antibodies and Characteristics Shared by ML Protein Group Members

Saori Ichikawa[1,2], Toshiro Takai[3,*], Takashi Inoue[3], Toshifumi Yuuki[3], Yasushi Okumura[3], Kenji Ogura[2,†], Fuyuhiko Inagaki[2,†] and Hideki Hatanaka[2,‡,§]

[1]Department of Material and Biological Sciences, Faculty of Science, Japan Women's University, Mejirodai, Bunkyo-ku, Tokyo 112-8681; [2]The Department of Molecular Physiology, Tokyo Metropolitan Institute of Medical Sciences, Honkomagome, Bunkyo-ku, Tokyo 113-8613; and [3]Bioscience Research and Development Laboratory, Asahi Breweries, Ltd., 1-1-21, Midori, Moriya, Ibaraki 302-0106

Received September 21, 2004; accepted November 3, 2004

Group 2 major mite allergens Der f 2 and Der p 2 are classified into the recently identified group of MD-2-related lipid-recognition (ML) proteins, but the ligands and biological functions of these allergens are unknown. We have obtained a high-quality NMR structure for Der f 2, and found that it is more similar to the crystal structure of NPC2, a distant homologue, than to that of Der p 2, in terms of the separation and angle between the two major β-sheets. This made us propose that ML proteins undergo clamshell-like motions that change the sizes of ligand-binding spaces inside their immunoglobulin-fold β-sandwich to accommodate lipid molecules. This type of motion in lipopolysaccaride recognition of MD-2 is suggested to be likely as well by structural models. We also report the applicability of NMR differential exchange broadening experiments for complexes of intact monoclonal antibodies and antigens; using this technique, we have detected the conformational epitopes for monoclonal antibodies 15E11 and 13A4 as two separate surface patches.

Key words: allergens, immunoglobulin fold, lipid binding, nuclear magnetic resonance, protein structures.

Abbreviations: LPS, lipopolysaccharide; ML, MD-2-related lipid-recognition; NOE, nuclear Overhauser effect; RMSD, root mean square difference; TLR4, Toll-like receptor 4.

House dust mites *Dermatophagoides farinae* and *D. pteronyssinus* are recognized as major causes of heavy atopic diseases such as asthma and dermatitis. Among their proteins, the group 2 allergens Der f 2 and Der p 2, whose sequences are 88% identical, show the highest positive rates for atopic patients (*1*). But the reason why the group 2 allergens show so strong allergenicity is unknown, although they are the best immunologically characterized allergens. Even their biological functions in mites are not yet known; however, we discovered Der f 2 binds to the bacterial surface and suspected its involvement in antibacterial defense (*2*), and other groups later reported that its mammalian distant homologue, NPC2, binds cholesterol (*3*) and that it is responsible for Niemann-Pick type C2 disease, which is characterized by defective egress of cholesterol from lysosomes (*4*).

Recently the group 2 mite allergens and NPC2, together with other more distantly-related proteins such as MD-2 and GM2-activator protein, were reported to form a novel group named ML (MD-2-related lipid-recognition), and this group was suggested to be involved in innate immunity and lipid metabolism (*5*). The representative protein in mammals, MD-2, forming a complex with Toll-like receptor 4 (TLR4), is essential for innate immune responses against bacterial lipopolysaccharide (LPS) (*6*), and was recently demonstrated to bind the lipid A portion of LPS (*7*).

The tertiary structure of ML proteins was first determined for Der f 2 by NMR and found to be a single-domain β-sandwich protein of immunoglobulin fold (*2*), which was later confirmed for Der p 2 by NMR (*8*). But the next determined ML structure revealed that GM2-activator protein adopts a cup-shaped eight-stranded β-sheet, named a β-cup fold (*9*), unlike the group 2 mite allergens, and its structure comprises an independent fold group within protein structure classification databases such as SCOP (*10*) even after the ML group was established. When the structure of Der p 2 was determined by X-ray crystallography with a quality higher than for the two previous NMR structures, its overall structure was found to be similar to them, but the two β-sheets were further apart, with an unknown ligand being kept in a large hydrophobic cavity between the sheets (*11*). The crystal structure of NPC2, determined in the

[*]Present address: Atopy (Allergy) Research Center, Juntendo University School of Medicine, 2-1-1, Hongo, Bunkyo-ku, Tokyo 113-8421.
[†]Present address: Division of Structural Biology, Graduate School of Pharmaceutical Sciences, Hokkaido University, Kita-ku, Sapporo 060-0812.
[‡]Present address: Graduate School of Systems Life Sciences, Kyushu University, Hakozaki, Higashi-ku, Fukuoka 812-8581.
[§]To whom correspondence should be addressed at the present address. Tel: +81-92-642-6969, Fax: +81-92-642-6764, E-mail: hideki@sls.kyushu-u.ac.jp

absence of cholesterol, had the same fold as the group 2 allergen structures, with separation between the sheets similar to the NMR structures (*12*).

In this study, we report the high-quality NMR structure of Der f 2, determined with a new sample, new NOESY spectra, and almost twice as many long-range distance restraints as in our previous structure determination. The refined Der f 2 structure was more alike to the NPC2 crystal structure than that of Der p 2 in terms of the separation and angle between the two major β-sheets. This made us propose that the accommodation of lipid molecules is enabled by clamshell-like motions of the immunoglobulin fold β-sandwich of ML proteins. The motion on LPS recognition of MD-2 is discussed using structural models. We also report the feasibility of NMR differential exchange broadening experiments for intact monoclonal antibodies, which are considered difficult due to their tight binding to antigens.

EXPERIMENTAL PROCEDURES

Sample Preparation—Escherichia coli BL21(DE3) cells harboring pFLT1 (pGEMEX1 derivative containing cDNA for clone 1 of Der f 2; see (*13*)) were cultured in M9 minimum medium in the presence of [^{13}C]glucose and [^{15}N]ammonium chloride. Labeled recombinant Der f 2 was expressed and purified as described (*14*). For structure refinement, 2.7 mM Der f 2 was dissolved in buffer comprising 20 mM KH_2PO_4/Na_2HPO_4 (pH5.6), 140 mM *n*-octyl-β-D-glucoside, 0.01% (w/v) NaN_3, 90% (v/v) H_2O, and 10% (v/v) D_2O. For binding experiments, purified ^{15}N-labeled recombinant Der f 2 was dissolved at 0.3 mM in buffer comprising 20 mM KH_2PO_4/Na_2HPO_4 (pH 5.6), 0.01% (w/v) NaN_3, 60 mM *n*-octyl-β-D-glucoside, 90% (v/v) H_2O, and 10% (v/v) D_2O. Two anti-Der f 2 mouse IgG mAbs, 15E11 and 13A4, were prepared from BALB/c mice as described previously (*15*), and suspended at 0.73 mM in buffer comprising 20 mM KH_2PO_4/Na_2HPO_4 (pH 5.6) and 0.01% (w/v) NaN_3.

NMR Spectroscopy—For structure refinement, NMR spectra were acquired at 55°C with a Varian Unity*plus* 600 NMR spectrometer equipped with a triple resonance pulse field gradient probe. Nuclear Overhauser effects (NOEs) were derived from three-dimensional ^{15}N-edited and ^{13}C-edited NOE spectroscopy spectra (*16*) recorded with a mixing time of 60ms.

For binding experiments, two-dimensional ^{1}H/^{15}N-HSQC (*16*) spectra of Der f 2 were acquired at 40°C with a Varian Unity*plus* 600 NMR spectrometer, operating at 600 MHz for ^{1}H. Each unlabeled mAb was added to the Der f 2 solution containing detergent as described above and spectra were collected at several mAb concentrations. The spectral widths were 9,000.9 and 2,099.9 Hz in the F2 and F1 dimensions, respectively. The data were sampled with 1,088 and 64 complex points at t2 and t1, respectively. Each t1 slice was the sum of 128 scans. The data were zero filled to a final size of 2,048 × 512 and a gaussian function was applied in both dimensions. The amplitudes of the cross peaks were measured using standard Varian software (VnmrX). In order to correct for the difference in the unknown concentration of free Der f 2 between samples, we first sorted the HSQC crosspeaks according to the ratio [Amplitude with 15E11]/[Amplitude with 13A4] and made a bar graph. Then we found that the height of the plateau equaled their median 1.20, and that 65% of the ratios were within 0.10 from 1.20. So [Amplitude with 15E11] – 1.20 × [Amplitude with 13A4] was used as the (normalized) peak intensity difference. The error of amplitudes was estimated from the noise level.

Structure Calculations—Upper limits of distance constraints were calculated as $kI^{-1/6}$, where I is the peak intensity and k is a constant adjusted for each NOE spectroscopy spectrum and relaxed by 0.5 Å considering mobility. Lower limits of distance constraints were all 1.8 Å. The structures were calculated with X-PLOR ver. 3.1 (*17*). Initial coordinates were generated using random ϕ and ψ angles, whereas peptide bonds and side-chains had extended conformations. The macroprogram sa.inp in X-PLOR ver. 2.1 was used to carry out simulated annealing calculations. The target function that is minimized during simulated annealing comprises only potential terms for covalent geometry, experimental distance restraints, experimental dihedral angle restraints, and van der Waals nonbonded repulsion. No hydrogen bonding, electrostatic, or 6–12 Lennard-Jones potential terms were present in the target function. The final structure calculations were based on 1,693 interproton distance restraints (588 intra-, 311 sequential ($|i-j|=1$), 155 middle range ($2 \le |i-j| \le 5$), and 477 long range ($|i-j| > 5$) NOEs). In addition, 161 constraints were assigned to multiple pairs using X-PLOR "or" operators and dynamically assigned to each pair during structural calculations, and 132 dihedral angle constraints were derived from TALOS (*18*).

A final set of 10 converged structures was selected from 100 calculations on the basis of agreement with the experimental data and van der Waals energy. A mean structure was obtained by averaging the coordinates of the structures that were superimposed in advance to the best converged structure and then minimizing under the constraints.

RESULTS

Structure Refinement—We refined the NMR structure of Der f 2 by using a highly concentrated sample and new NOESY spectra. The number of long-range distance restraints derived from newly measured 3D ^{15}N-edited and ^{13}C-edited NOESY spectra was 477, which is much larger than that of our previous work, 246 (*2*). Since we used the same sample buffer and temperature, the chemical shifts did not change essentially, but we could add assignments for W92 $H^{\varepsilon 1}$ and $N^{\varepsilon 1}$, whose peaks had been too weak to detect previously, perhaps due to fast solvent exchange. We also detected a hydroxyl proton, T47 $H^{\gamma 1}$, at 6.94 ppm. In addition, we were able to determine that only P79 out of the six prolines is a *cis*-proline from the chemical shift differences of C^{β} and C^{γ} (*19*).

Table 1 summarizes the statistics for the set of the 10 final structures and for the mean structure, and shows, for example, that the number of distance constraint violations above 0.3 Å ranged from 1 to 3, and that the deviation from ideal bond lengths was 0.004 Å. These figures represent a relatively good quality of the structure refinement, considering that our distance constraint set was tighter than those in the typical three level classifi-

Table 1. **Structural statistics.** <SA> refers to the final set of simulated annealing structures and $(SA)_r$ is the mean structure. The numbers of terms are given in parentheses.

Parameter	<SA>	$(SA)_r$
RMSDs from experimental distance constraints (Å) (1693)	0.034 ± 0.002	0.031
Number of distance constraint violations greater than 0.3 Å	1–3	2
Maximum (Å)	0.52	0.38
RMSDs from experimental dihedral constraints (deg) (128)	4.4 ± 0.2	4.3
F_{NOE} (kcal/mol)[a]	95.4 ± 9.9	83.283
F_{CDIH} (kcal/mol)[a]	38.3 ± 4.2	35.993
F_{repel} (kcal/mol)[a]	39.8 ± 4.4	28.930
RMSDs from idealized geometry		
Bonds (Å) (1995)	0.004 ± 0.000	0.003
Angles (degrees) (3644)	0.69 ± 0.01	0.633
Impropers (degrees) (994)[b]	0.51 ± 0.02	0.414

[a]The value of the square-well NOE potential, F_{NOE}, is calculated with a force constant of 50 kcal/mol per Å^2. The value of F_{repel} is calculated with a force constant of 4 kcal/mol per Å^2 with the van der Waals radii scaled by a factor of 0.8 of the standard values used in the CHARMm empirical function. [b]The improper torsion term is used to maintain the planar geometry and chirality.

cation (*20*). In the Ramachandran plot made with PROCHECK (*21*), 79.8%, 17.0%, 3.3% and 0.0% of the residues were in the core, allowed, generously allowed and disallowed regions, respectively, which also supports the good stereochemistry of the refined structure. The root mean square difference (RMSD) of the 10 final structures from the minimized averaged structure was 0.50 ± 0.08 Å for the backbone (N, C$^\alpha$, C′) atoms of all residues 1–129, and 0.92 ± 0.12 Å for the non-hydrogen atoms of the same residue range. These RMSD values indicate that the structural convergence is high enough for the discussion below.

Description of the Structure—Figure 1 shows the refined structure of Der f 2. We confirmed our previous report (*2*) that Der f 2 adopts an immunoglobulin-fold of the s-type (*22*). However, the angles made by the β-strands of one sheet and those of the other changed: they are constantly about 30° in the current refined structure, although in our previous structure they varied from about 30° to almost 0° along the strands. Distance restraints for the residue pairs 52–90, 54–92, 65–92 and 65–95 are inconsistent with the old inter-strand angle, being responsible for the angle change. In addition, some improvements were made at one end of the molecule (Fig. 1b) where we

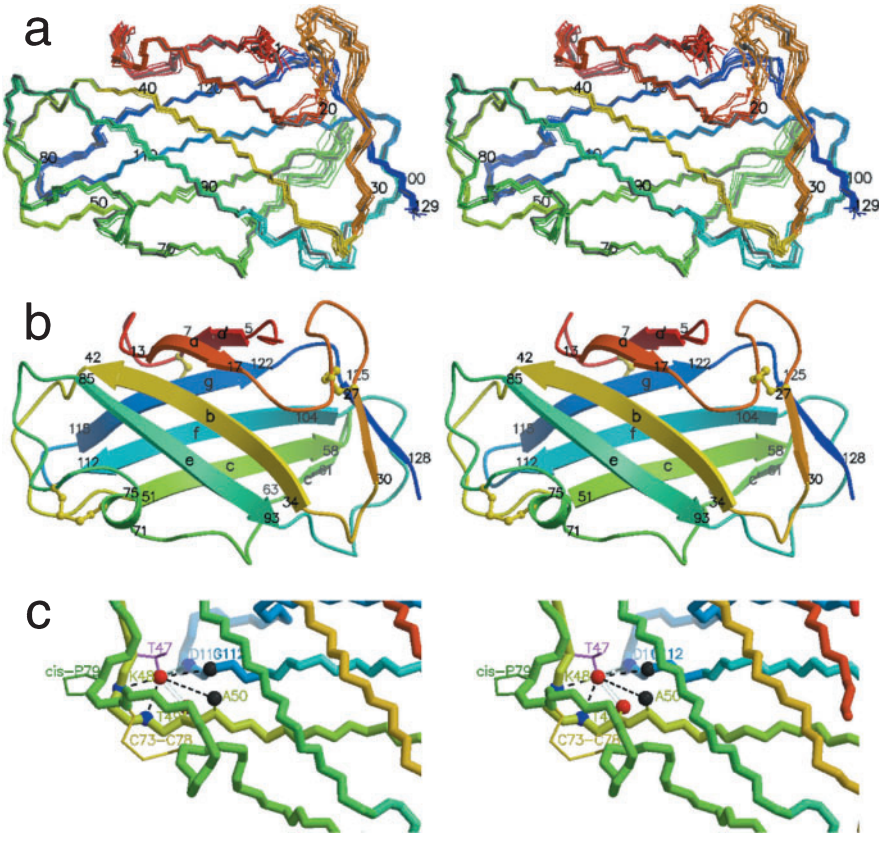

Fig. 1. **Stereo views of the refined tertiary structure of Der f 2.** (a) Best fit superposition of the backbone atoms (N, C$^\alpha$, C′) of the 10 final structures of Der f 2. Amino acid residue numbers are shown every ten residues. (b) Ribbon diagrams of the mean structure of Der f 2. The start and end residue numbers of the β-strands are also shown. Disulfide bonds are colored yellow. Both figures were generated with MOLSCRIPT (*35*) and RASTER3D (*36–38*). The color changes from red (N terminus) to blue (C terminus). (c) A close-up for T47, the only threonine residue whose hydroxyl proton H$^{\gamma 1}$ was observed. Black dashed lines show NOEs from the T47 H$^{\gamma 1}$, and cyan transparent tubes show probable hydrogen bonds formed by O$^{\gamma 1}$. Some carbon, nitrogen and oxygen atoms are shown as black, blue and red spheres, respectively.

Table 2. **Structural comparison among Der f 2, Der p 2 and NPC2.**

	Der f 2	Der p 2 (NMR)	Der p 2 (X-ray)	NPC2
Der f 2	–	1.63 Å (95)	1.61 Å (124)	1.42 Å (118)
Der p 2 (NMR)		–	1.64 Å (97)	1.66 Å (89)
Der p 2 (X-ray)			–	1.52 Å (119)
NPC2				–

The RMSD values for pairs of structures were calculated automatically with the program SHP (*23*) for the C^{α} atoms that could be fitted within 3 Å. The numbers of fitted C^{α} atoms are shown in parentheses.

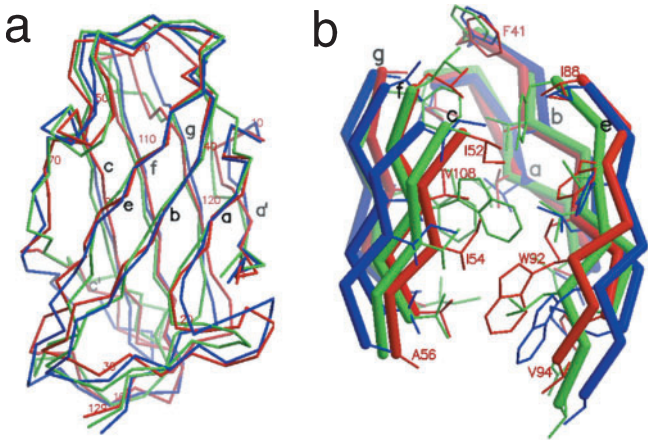

Fig. 2. **Superposition of Der f 2 and related structures.** (a) Superposition of the C^{α} traces of Der f 2 (red), Der p 2 in crystal (blue) (*11*), and NPC2 (green) (*12*). Large β-strands are labeled and Der f 2 is numbered every ten residues. (b) The central region of the immunoglobulin-fold β-sandwich. Internal side chains are also shown as thin lines and some of them are labeled. Strands c and f, and the C-terminal half of e of Der f 2 and NPC2 are shifted toward the inside compared to those of Der p 2 (blue).

can now define another β-sheet made of residues 27–30 and 125–128, which is much smaller and also found in the crystal structure of Der p 2 (*11*).

Our refined structure enabled clear determination of the details, such as a 3_{10} helix at N71–F75 and the only *cis*-proline P79. At the same end of the molecule, the detectable hydroxyl proton T47 $H^{\gamma 1}$ gave strong NOE peaks with K48 H^{N}, T49 H^{N}, A50 H^{β}, G112 H^{α} and D113 H^{N}, which suggest that hydrogen bonds are formed at T47 $H^{\gamma 1}$–T49 O and T47 $O^{\gamma 1}$–D113 H^{N}. This hydrogen bond network appears to make T47 the only threonine residue that orients its sidechain toward the molecule's interior. This end of the molecule, better defined by NMR, seems to be made rigid by all these local characteristics described above, together with the disulfide bond C73–C78.

By contrast, the other end of the molecule is less defined (Fig. 1a) and appears to be loosely packed. This looseness is caused by the absence of inter-sheet NOE restraints in some regions of the two large sheets: the residues in one sheet I13, V16, V18, F35 and A39 make no restraints with the other large sheet, and vice versa for A56, I58, V104, V108, A120 and A122.

Structural Comparisons with Other Structures—We compared our structure with the three available homologue structures (*8*, *11*, *12*). We first calculated structural similarity automatically with SHP (*23*) (Table 2). This table shows that many fewer residues could be superimposed between the Der p 2 NMR structure and the others. The fact that Der p 2 segments 18–21, 26–37, 60–66, 70–77, 88–97 and 125–129 could not be matched correctly between the X-ray and NMR structures suggests that it is inappropriate to include this structure for detailed comparison.

Our Der f 2 structure, the Der p 2 X-ray structure and the NPC2 structure are similar to each other (Table 2 and Fig. 2a), in spite of the low sequence similarity between NPC2 and the two mite allergens (about 25%). The numbers of insertions and deletions in NPC2 well explain the decreases in the numbers of matched residues, and therefore we suggest the RMSD values simply reflect the extents of structural similarity. This means that the similarity of our Der f 2 structure to that of NPC2 is significantly higher than the similarity between the other pairs.

One of the main differences between our Der f 2 NMR structure and the Der p 2 crystal structure is the separation between the two major β-sheets. When superimposed globally, strands c and f, and the C-terminal half of e of the Der f 2 NMR structure are shifted toward the inside (Fig. 2b), by 3.3, 2.8 and 2.6 Å maximally, at residues I54, V108 and V94, respectively. Many NOEs inconsistent with the Der p 2 crystal structure, for example, the NOE networks for the residue pairs 54–90 and 52–90, support the shifting of these strands. However, β-strands a, b and g occupy similar positions in both structures. Thus the two major β-sheets make different angles like a clamshell (Fig. 3, a and b).

Accordingly, the sizes of the cavities between the sheets are different in these two structures. In the Der p 2 crystal structure (Fig. 3b), a huge cavity occupies the space between the sheets, which has a tunnel leading to the outer space. It is rimmed by segments 61–67 (strand c′ and the following sequence) and 91–99 (loops e–f). We call this site the mouth of the cavity hereafter. In contrast, our Der f 2 NMR structure has two small separated cavities (Fig. 3a), a larger one deep inside and a tiny one at the mouth. These cavities are separated by the motion of strands c and f, and the cavity deep inside remains uncorrupted because the β-strands a and b do not move. Thus the changes in the cavities are well explained by the clamshell-like motion described above.

The other difference is in the shape of the β-sandwich edges forming the mouth of the cavity (Fig. 3, a and b). In the Der f 2 NMR structure segment 91–99 shifts toward segment 61–67. This makes the mouth of the cavity narrower in the Der f 2 NMR structure. In the Der p 2 crystal structure D64, next to β-strand c′, is detached from strand c around residue D64 and shifted by 3.4 Å in the global superimposition.

The clamshell-like change of the β-sandwich is clearly seen when all the ML proteins with known structures are compared with each other (Fig. 3). The NPC2 crystal structure is similar to our Der f 2 NMR structure in terms of the angle made by the two β-sheets (Fig. 3c). NPC2 has only a very tiny cavity inside according to GRASP (*24*), different from Der f 2, but this is due to substitutions of aromatic residues for small hydrophobic

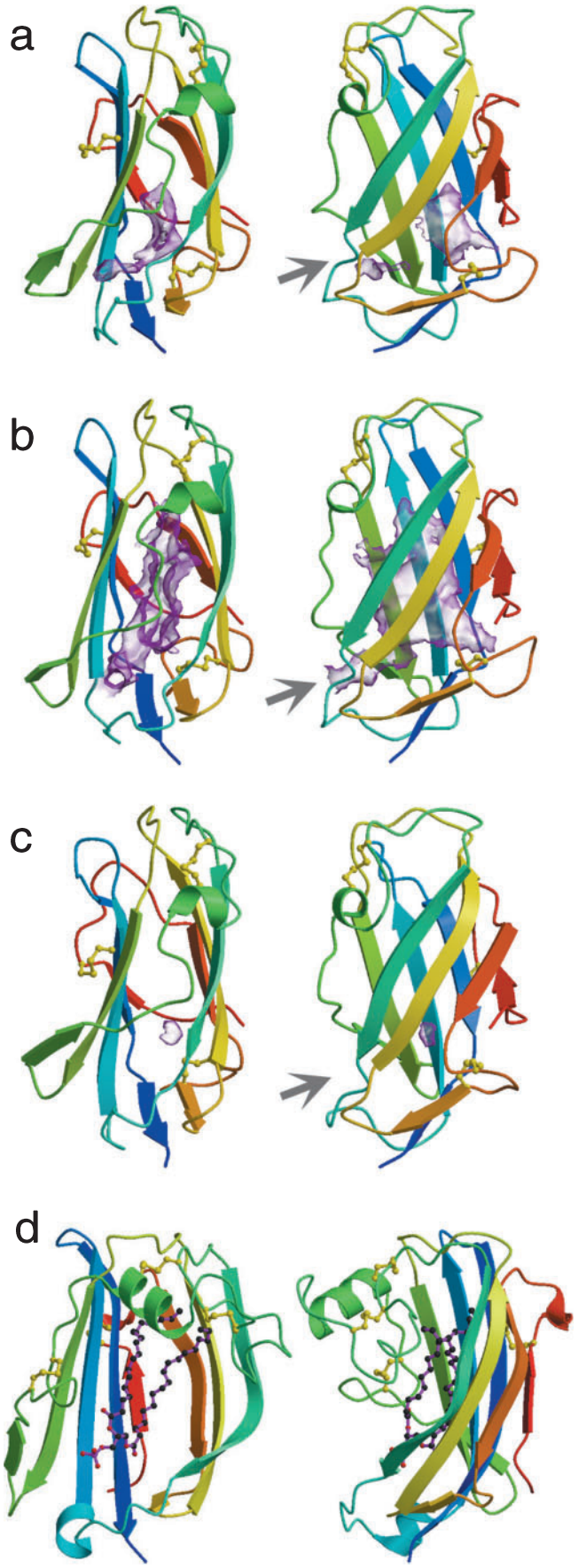

ones. The radically opened structure of GM2-activator (Fig. 3d) will be explained under "DISCUSSION."

Antibody Binding Experiments—We also performed differential exchange broadening experiments to detect monoclonal antibody epitopes (Fig. 4). Because we had expected difficulty in NMR detection of epitopes for intact antibodies due to the sizes of the complexes being inappropriate for chemical shift perturbation experiments (above 150 kDa) and to the binding strength being inappropriate for exchange broadening detection (K_d = 50 pM and $k_d = 8.3 \times 10^{-6}$ s^{-1} for 15E11, and K_d = 1.8 nM and $k_d = 4.4 \times 10^{-4}$ s^{-1} for 13A4, preliminarily measured using BIAcore), we tried detecting exchange broadening in the presence of detergent, expecting weakened binding strengths of the antigen/antibody complexes. With 60 mM *n*-octyl-β-D-glucoside and 40°C, we could easily observe ^{1}H-^{15}N HSQC signals (Fig. 4a) even after adding 13A4 up to the molar ratio 0.5:1 to Der f 2, which shows the detergent weakened the binding to the submilimolar K_d level, and, supposing the association was not accelerated, the k_d is considered to be above 10 s^{-1}. This indicates the dissociation and association of 13A4 were fast enough to detect exchange broadening in the presence of detergent. In contrast, when 15E11 was added instead of 13A4 at the molar ratio 0.5:1, all the cross peaks diminished, showing much stronger binding even in the presence of the detergent. However, at the molar ratio of 0.375:1, the remaining cross peaks were found to be attenuated differently peak by peak, suggesting exchange broadening. The chemical shifts of peaks in both cases were almost the same as those in the absence of mAbs, so their assignments were easily established.

For some backbone amides (Fig. 4b) and sidechain carboxamides (Fig. 4c), significant peak intensity differences were observed between the HSQC spectra with the molar ratios of Der f 2:15E11 = 1:0.375 and Der f 2:13A4 = 1:0.5. The amplitudes of 12 amides (D19, K48, T49, I54, A56, V65, D69, N71, K77, Y86, L110 and N114) and 2 carboxamides (N71 and Q84) were lower for 15E11, and those of 12 amides (Q2, A9, N10, N11, H22, I29, K33, L61, E62, K100, S101 and R129) and 3 carboxamides (N10, N11 and N103) were lower for 13A4. These two groups of locations were together on the separate surface regions of Der f 2 (Fig. 4d), except for D19. This clear distribution made us conclude that these two regions correspond to the epitopes for 15E11 and 13A4, respectively, considering that 15E11 and 13A4 have been shown to bind a Der f 2 molecule simultaneously in sandwich ELISA experiments (*25*). We also compared the spectrum in the absence of mAbs and that with 15E11 or 13A4, but in both cases the locations exhibiting peak amplitude differences failed to make up a region on the tertiary structure

Fig. 3. **Structural comparison of ML proteins.** Ribbon diagrams are shown, with views related by 90° rotation. (a) Der f 2; (b) Der p 2 in crystal (*11*); (c) NPC2 (*12*); (d) GM2-activator (*28*). Secondary structure elements are colored as in Fig. 1b, and internal cavities calculated with a probe radius of 1.4 Å are also shown in magenta, using GRASP (*24*). In (b), the cavity is connected with the exterior through a short tunnel, and this position, called the mouth of the cavity in the text, is shown by gray arrows in (a)–(c). In (d), no cavities exist, and, instead, the bound ceramide moiety is shown in ball-and-stick representation.

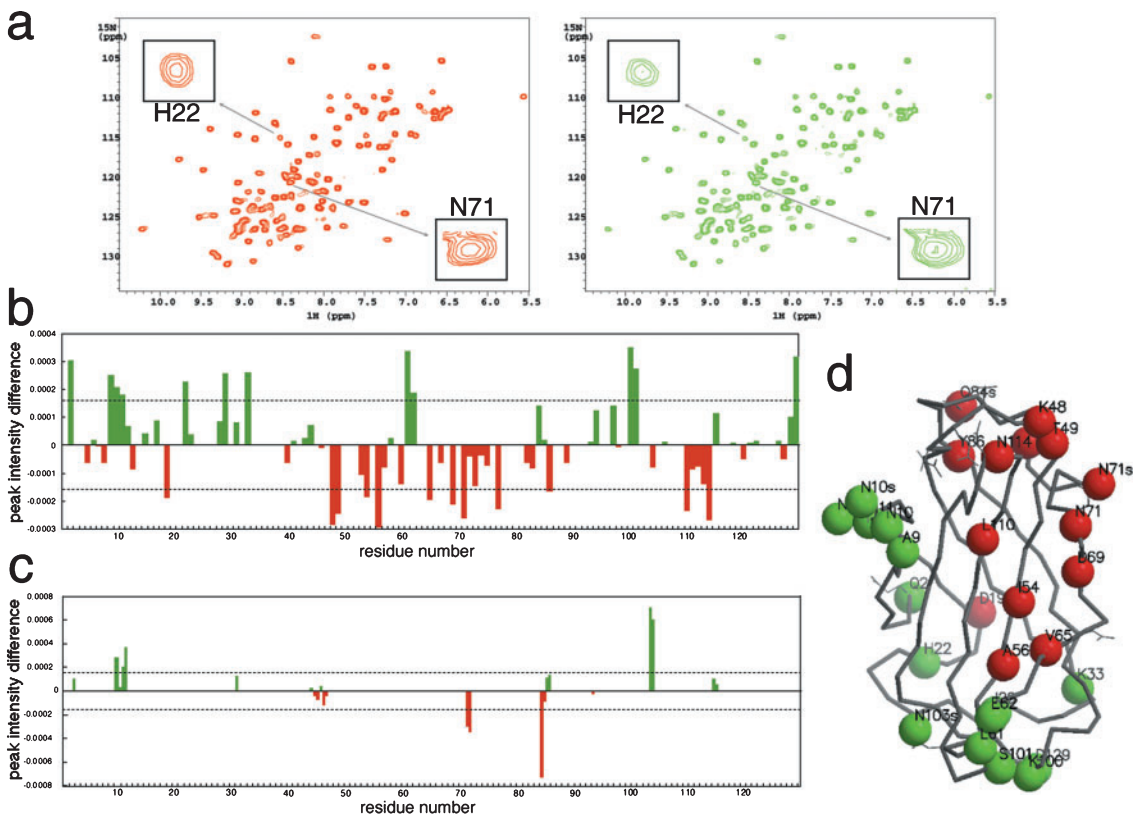

Fig. 4. **Epitope mapping for mAbs by NMR differential exchange broadening.** (a) HSQC spectra of Der f 2 mixed with mAbs at the molar ratios of Der f 2:15E11 = 1:0.375 (red) and Der f 2: 13A4 = 1:0.5 (green). The latter spectrum is amplified by a normalization factor of 1.20, considering the estimated concentration ratio of mAb-free Der f 2. Insets show close-ups of peaks showing exchange broadening. (b and c) The peak amplitude differences between the two HSQC spectra calculated after normalization. (b) Amide protons; (c) carboxamide protons. The unit is spectrometer-defined. The broken line shows the error level. (d) Epitope maps for 15E11 (red) and 13A4 (green), made by coloring the nitrogen atoms where negative and positive significant peak amplitude differences, respectively, were observed in (b) and (c).

of Der f 2 (data not shown), possibly due to the effects of decreases in the detergent concentrations during mAb additions.

DISCUSSION

Clamshell-Like Motion of the Immunoglobulin-Like Fold of ML Proteins—We have obtained a high-quality NMR structure of Der f 2 (Table 1 and Fig. 1), which we found was distinct from the crystal structure of Der p 2 (*11*), a homologue exhibiting 88% sequence identity (Table 2 and Fig. 2). Although structural multiplicity had been suggested for these proteins (*11*), our refined structure has provided the first opportunity to discuss in detail the closed form of group 2 mite allergens (Fig. 3). The most significant difference between the two structures was the angle made by the two major β-sheets, so we concluded the group 2 mite allergens can undergo a clamshell-like motion upon ligand binding.

The backbone structure of our structure was essentially the same as that of a distantly homologous cholesterol-binding protein, NPC2 (*12*), which we regard as the closed form too. As suggested in (*12*), NPC2 has to open its β-sheet like the Der p 2 crystal structure to accommodate cholesterol, since there are no cavities large enough.

GM2-activator was found to have a novel fold named β-cup when its structure was determined (*9*), but it was later classified into a novel protein group, ML, as well as the group 2 mite allergens and NPC2 by extensive sequence comparisons (*5*). Figure 3 supports the latter classification; although GM2-activator has a very different shape, the topology of its secondary structure elements is exactly the same as those of the other ML proteins, and each of the two conserved disulfide bonds plays a similar role in the global structure. Thus the fold of GM2-activator can be considered to be essentially the same as the immunoglobulin fold, whose clamshell is radically opened, regardless of ligand binding.

Considering these together with the discussion on MD-2 below, we suggest that ML proteins open their immunoglobulin fold β-sandwich like a clamshell, when necessary.

Structural Models of Opening and Closure of MD-2 Protein—MD-2, a key molecule in innate immunity, is the most representative member of the ML protein group. Although its tertiary structure has not been determined, a structural model of it was presented very recently (*26*). However, this model is based on mixed information from the open and closed forms, and one of them, the Der p 2 NMR structure, is the most different from the other ML structures (Table 2). So we built refined models of human

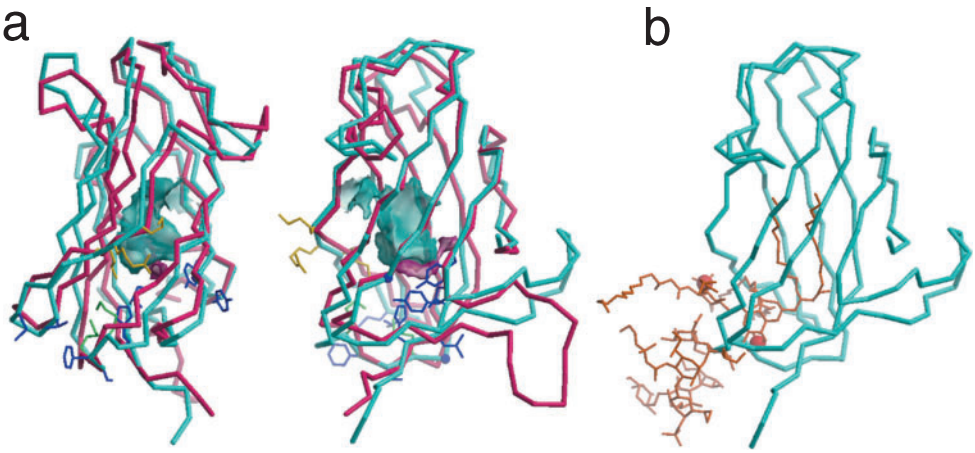

Fig. 5. **Two structural models of MD-2 in open and closed forms.** (a) Superposition of the C^{α} traces and inner cavities of MD-2 models made with Der f 2 (magenta) and Der p 2 in crystal (sky blue) as modeling templates. Comparative modeling program MODELLER version 6v2 (*39*) with default parameters was able to generate models without large steric hindrance. The right view can be related to the left by 90° *y* rotation. The sidechains of K71, R72 and K73 are colored yellow, and those of K107 and K110 are colored green. Blue sidechains represent Y16, Y18, G41, V64, M67, F108, S109, G111, I135, L136 and H137. (b) A very rough model of the MD-2/LPS complex. Conformation editing of LPS (orange) and its docking to the open MD-2 model (sky blue) were performed manually. The phosphate groups of lipid A are shown as spheres.

MD-2 in the open and closed conformations using our improved NMR structure of Der f 2 and the crystal structure of Der p 2, respectively, as modeling templates.

These two MD-2 models (Fig. 5a) are different from each other. The most conspicuous difference between them is at the large disulfide-bonded loop C19–C33, but we regard this is groundless because this loop includes an insertion of 8 or 9 residues lacking any structural information. The second one is the distances of β-strands c and f from the β-sheet opposite, which is based exactly on the opening and closure of the template structures. The closed MD-2 model has only tiny cavities, but the open MD-2 model has a large cavity, which we expect corresponds to the binding site of the lipid A portion of lipopolysaccharide.

There are some important differences between our two MD-2 models and the model previously reported (*26*). For example, the positive charge cluster K71, R72 and K73 (we number MD-2 supposing its signal peptide is 18 residues long) showed a shift in its Cα position by 4.6–5.9 Å (data not shown), and in our human MD-2 models this cluster makes contact with another positive charge cluster including K104, K107, K110, K112, K114, K37 and K40. These two clusters were each mutated at multiple residues K71–K73 and K107/K110 (yellow and green in Fig. 5a, respectively), and both mutants largely impaired LPS signaling in the same modeling paper (*26*). This displacement is mainly due to the two-residue shift of the five MD-2 residues P70–E74 (Der f 2 D64–I68 in our sequence alignment (Fig. 6)), which is reasonable considering the strand c' location common in the two high-quality template structures and in the NPC2 structure.

The conserved cavity makes us believe that the acyl groups of LPS lipid A bind in the cavity, similar to the two fatty acid-like electron densities found for the Der p 2 crystal structure (*11*). This belief is consistent with the results of alanine-scanning experiments, in which several mutations changing the cavity wall (blue sidechains in Fig. 5a) decreased LPS signaling without affecting binding to TLR4 (*27*). The positive charges at K71–K73 and K107/K110 are, in turn, close to the region corresponding to the mouth of the cavity found in the Der p 2 crystal, and probably contribute to binding to phosphate groups in LPS lipid A. In order to illustrate these points, we manually made a very rough model of a possible mode of binding of MD-2 and LPS complex (Fig. 5b). However, since it was difficult to avoid steric hindrance at the cavity mouth, it might have to open more to bind LPS, possibly through displacing the segment 69–74 or additional clamshell-like motion. Our model also took into account the ligand character and binding mode found for GM2-activator (Fig. 3d) (*28*). We have little information on which of the six acyl groups of lipid A binds to MD-2, and we suspect LPS might be multivalent, since LPS oligomerizes MD-2/TLR receptors (*29*), but oligomerization might be induced indirectly by MD-2 conformational changes, such as mentioned here.

Implied Biological Functions of Mite Group 2 Allergens—In contrast to LPS for MD-2 and cholesterol for NPC2, the ligand of the group 2 mite allergens has not been identified yet. Binding ability to bacterial surfaces (*2*), unidentified fatty acid–like electron density found inside Der p 2 produced by *E. coli* (*11*), and the existence of a large positive charge cluster (*2*) near the cavity mouth suggest that the group 2 mite allergens bind lipids from the bacterial surface carrying negative charges and acyl groups, such as LPS. The positive charge cluster of Der f 2 is composed of R31, K33, K96, K100, K126, R128 and possibly H30, if it functions at acidic pH. These residues are not conserved among ML proteins except R31 (Fig. 6), but the cluster exists in a similar region in MD-2, but not in NPC2, which also agrees with the idea of LPS binding. However, the residues surrounding the cavity are not conserved between Der f 2 and MD-2, so it is also possible that other negatively-charged lipids bind Der f 2. At least, we think the unidentified ligand in the Der p 2 (*11*) crystal is not LPS, considering crystal contacts between the molecules.

NMR Detection of Epitopes—We have detected the epitope regions of mAbs 13A4 and 15E11 by means of NMR (Fig. 4). The two sets of locations exhibiting differential exchange broadening were distributed separately (except for D19, see below), which shows the usefulness of our method, considering that sandwich ELISA experiments had shown these two mAbs can bind to Der f 2 simultaneously (*25*). We previously reported alanine sub-

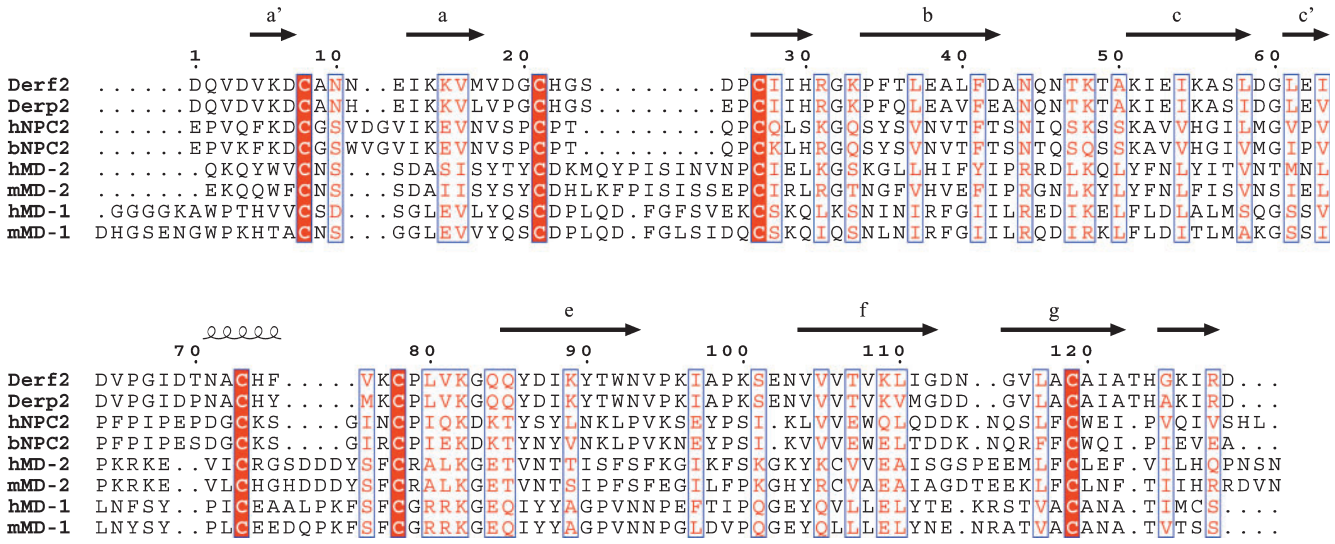

Fig. 6. **Sequence alignment of ML proteins.** The amino acid sequences of Der f 2, Der p 2, human NPC2, bovine NPC2, human MD-2, mouse MD-2, human MD-1 and mouse MD-1 were aligned using structural information, and shown using ESPript (*40*). The conserved cysteine residues are indicated by highlighted red boxes. Other type-conserved residues are colored red and enclosed by blue boxes. The secondary structure of Der f 2 (arrows indicate β-strands and the squiggle represents a helix) is shown above the sequences.

stitution experiments on 43 residues, and identified D69, N71 and H74 as epitope residues for 15E11, and R128 and D129 for 13A4 (*30*), which supports our current NMR results perfectly, taking into account that we observed mainly backbones and that alanine substitutions modified sidechains. Our results also match the facts that two other Der f 2 variants, clone 2 with only one substitution, V76M, and clone 11 with three substitutions, V76M, I88M and I111V, showed similar affinity to 13A4 but lower affinity to 15E11 (*31*).

In the Der f 2 structure, D19 is located apart from the region identified as the epitope of 15E11 (Fig. 4). We previously reported that substitutions D19A and D19N, but not D19E, weakened the binding ability to both 15E11 and to 13A4 (*30*). Considering the above together, we suggest that removal of the negative charge of D19 might affect the global antigenic character of Der f 2, and besides that binding of 15E11 or 13A4, in turn, might change the conformation or environment of D19.

Although we have elucidated the epitopes of two mAbs, more clones of antibodies or polyclonal antibodies need to be investigated to discuss the structure-antigenicity relationship. In addition, as to the structure-allergenicity relationship, IgE rather than IgG should be studied, which would be more difficult due to its lower concentration in sera.

We showed the applicability of detergent to the NMR detection of interfaces of large tight-binding complexes, such as those between antigens and intact antibodies (Fig. 4). This might lead to an alternative method of epitope mapping of polyclonal antibodies in sera, which is usually of greater interest, although, to date, monoclonal Fab or Fv have been amenable to NMR or crystallographic techniques. Hydrogen-protection NMR is also useful for intact antibodies, but its fidelity depends on several factors, and only small numbers of contact residues were detected when applied to Der p 2 (*32*). The cross-saturation method combined with the TROSY technique was recently developed to determine the interfaces of large complexes precisely (*33*). But, since all antigen crosspeaks perturbed by different polyclonal antibody molecules cannot be assigned, we have to use a modification of it, the transferred cross-saturation method (*34*), which also needs weak binding and fast dissociation. Our study demonstrated that detergents are advantageous for moderating the tight binding of antigen-antibody complexes. This knowledge leads us to expect that the combination of detergent and transferred cross-saturation might give the most precise epitope maps both for mAbs and, more hopefully, for polyclonal antibodies.

The atomic coordinates and distance restraints have been submitted to the Protein Data Bank and given the entry code 1WRF.

We wish to thank Namiko Iwamoto-Yasue and Midori Akagawa-Chihara (Asahi Breweries, Ltd.) for the technical advice. We also thank Drs. Hideoki Ogawa, Ko Okumura (Juntendo University School of Medicine), and Daisuke Kohda (Kyushu University) for the comments and encouragement.

REFERENCES

1. Heymann, P.W., Chapman, M.D., Aalberse, R.C., Fox, J.W., and Platts-Mills, T.A. (1989) Antigenic and structural analysis of group II allergens (Der f II and Der p II) from house dust mites (*Dermatophagoides* spp). *J. Allergy Clin. Immunol.* **83**, 1055–1067
2. Ichikawa, S., Hatanaka, H., Yuuki, T., Iwamoto, N., Kojima, S., Nishiyama, C., Ogura, K., Okumura, Y., and Inagaki, F. (1998) Solution structure of Der f 2, the major mite allergen for atopic diseases. *J. Biol. Chem.* **273**, 356–360
3. Okamura, N., Kiuchi, S., Tamba, M., Kashima, T., Hiramoto, S., Baba, T., Dacheux, F., Dacheux, J.L., Sugita, Y., and Jin, Y.Z. (1999) A porcine homolog of the major secretory protein of human epididymis, HE1, specifically binds cholesterol. *Biochim. Biophys. Acta* **1438**, 377–387
4. Naureckiene, S., Sleat, D.E., Lackland, H., Fensom, A., Vanier, M.T., Wattiaux, R., Jadot, M., and Lobel, P. (2000) Identifica-

tion of HE1 as the second gene of Niemann-Pick C disease. *Science* **290**, 2298–2301
5. Inohara, N. and Nunez, G. (2002) ML—a conserved domain involved in innate immunity and lipid metabolism. *Trends Biochem. Sci.* **27**, 219–221
6. Miyake, K. (2004) Innate recognition of lipopolysaccharide by Toll-like receptor 4-MD-2. *Trends Microbiol.* **12**, 186–192
7. Viriyakosol, S., Tobias, P.S., Kitchens, R.L., and Kirkland, T.N. (2001) MD-2 binds to bacterial lipopolysaccharide. *J. Biol. Chem.* **276**, 38044–38051
8. Mueller, G.A., Benjamin, D.C., and Rule, G.S. (1998) Tertiary structure of the major house dust mite allergen Der p 2: sequential and structural homologies. *Biochemistry* **37**, 12707–12714
9. Wright, C.S., Li, S.C., and Rastinejad, F. (2000) Crystal structure of human GM2-activator protein with a novel beta-cup topology. *J. Mol. Biol.* **304**, 411–422
10. Murzin, A.G., Brenner, S.E., Hubbard, T., and Chothia, C. (1995) SCOP: a structural classification of proteins database for the investigation of sequences and structures. *J. Mol. Biol.* **247**, 536–540
11. Derewenda, U., Li, J., Derewenda, Z., Dauter, Z., Mueller, G.A., Rule, G.S., and Benjamin, D.C. (2002) The crystal structure of a major dust mite allergen Der p 2, and its biological implications. *J. Mol. Biol.* **318**, 189–197
12. Friedland, N., Liou, H.L., Lobel, P., and Stock, A.M. (2003) Structure of a cholesterol-binding protein deficient in Niemann-Pick type C2 disease. *Proc. Natl Acad. Sci. USA* **100**, 2512–2517
13. Nishiyama, C., Fukada, M., Usui, Y., Iwamoto, N., Yuuki, T., Okumura, Y., and Okudaira, H. (1995) Analysis of the IgE-epitope of Der f 2, a major mite allergen, by *in vitro* mutagenesis. *Mol. Immunol.* **32**, 1021–1029
14. Iwamoto, N., Nishiyama, C., Yasuhara, T., Saito, A., Yuuki, T., Okumura, Y., and Okudaira, H. (1996) Direct expression of Der f 2, a major house dust mite allergen, in *Escherichia coli*. *Int. Arch. Allergy Immunol.* **109**, 356–361
15. Akagawa, M., Mori, T., Ando, T., and Okudaira, H. (1991) Preparation of specific monoclonal antibodies against Der f II one of the major allergens of *Dermatophagoides farinae*. *Arerugi* **40**, 1239–1242
16. Cavanagh, J., Fairbrother, W.J., Palmer, A.G., and Skelton, N.J. (1996) *Protein NMR spectroscopy. Principles and Practice*, Academic Press, San Diego, CA
17. Brunger, A.T. (1993) *X-PLOR Version 3.1: A System for X-ray Crystallography and NMR*, Yale University Press, New Haven, CT
18. Cornilescu, G., Delaglio, F., and Bax, A. (1999) Protein backbone angle restraints from searching a database for chemical shift and sequence homology. *J. Biomol. NMR* **13**, 289–302
19. Schubert, M., Labudde, D., Oschkinat, H., and Schmieder, P. (2002) A software tool for the prediction of Xaa-Pro peptide bond conformations in proteins based on 13C chemical shift statistics. *J. Biomol. NMR* **24**, 149–154
20. Kohda, D., Terasawa, H., Ichikawa, S., Ogura, K., Hatanaka, H., Mandiyan, V., Ullrich, A., Schlessinger, J., and Inagaki, F. (1994) Solution structure and ligand-binding site of the carboxy-terminal SH3 domain of GRB2. *Structure* **2**, 1029–1040
21. Laskowski, R.A., MacArthur, M.W., Moss, D.S., and Thornton, J.M. (1993) PROCHECK: a program to check the stereochemical quality of protein structures. *J. Appl. Crystallogr.* **26**, 283–291
22. Bork, P., Holm, L., and Sander, C. (1994) The immunoglobulin fold. Structural classification, sequence patterns and common core. *J. Mol. Biol.* **242**, 309–320
23. Stuart, D.I., Levine, M., Muirhead, H., and Stammers, D.K. (1979) Crystal structure of cat muscle pyruvate kinase at a resolution of 2.6 Å. *J. Mol. Biol.* **134**, 109–142
24. Nicholls, A., Sharp, K.A., and Honig, B. (1991) Protein folding and association: insights from the interfacial and thermodynamic properties of hydrocarbons. *Proteins* **11**, 281–296
25. Akagawa, M., Mori, T., Ando, T., and Okudaira, H. (1992) Specific measurement of a major mite allergen, Der f II, by an enzyme-linked immunosorbent assay system using monoclonal anti-Der f II antibodies. *Biosci. Biotechnol. Biochem.* **56**, 1725–1727
26. Gruber, A., Mancek, M., Wagner, H., Kirschning, C.J., and Jerala, R. (2004) Structural model of MD-2 and functional role of its basic amino acid clusters involved in cellular lipopolysaccharide recognition. *J. Biol. Chem.* **279**, 28475–28482
27. Kawasaki, K., Nogawa, H., and Nishijima, M. (2003) Identification of mouse MD-2 residues important for forming the cell surface TLR4-MD-2 complex recognized by anti-TLR4-MD-2 antibodies, and for conferring LPS and taxol responsiveness on mouse TLR4 by alanine-scanning mutagenesis. *J. Immunol.* **170**, 413–420
28. Wright, C.S., Zhao, Q., and Rastinejad, F. (2003) Structural analysis of lipid complexes of GM2-activator protein. *J. Mol. Biol.* **331**, 951–964
29. Visintin, A., Latz, E., Monks, B.G., Espevik, T., and Golenbock, D.T. (2003) Lysines 128 and 132 enable lipopolysaccharide binding to MD-2, leading to Toll-like receptor-4 aggregation and signal transduction. *J. Biol. Chem.* **278**, 48313–48320
30. Nishiyama, C., Hatanaka, H., Ichikawa, S., Fukada, M., Akagawa-Chihara, M., Yuuki, T., Yokota, T., Inagaki, F., and Okumura, Y. (1999) Analysis of human IgE epitope of Der f 2 with anti-Der f 2 mouse monoclonal antibodies. *Mol. Immunol.* **36**, 53–60
31. Nishiyama, C., Yuuki, T., Usui, Y., Iwamoto, N., Okumura, Y., and Okudaira, H. (1994) Effects of amino acid variations in recombinant Der fII on its human IgE and mouse IgG recognition. *Int. Arch. Allergy Immunol.* **105**, 62–69
32. Mueller, G.A., Smith, A.M., Chapman, M.D., Rule, G.S., and Benjamin, D.C. (2001) Hydrogen exchange nuclear magnetic resonance spectroscopy mapping of antibody epitopes on the house dust mite allergen Der p 2. *J. Biol. Chem.* **276**, 9359–9365
33. Takahashi, H., Nakanishi, T., Kami, K., Arata, Y., and Shimada, I. (2000) A novel NMR method for determining the interfaces of large protein-protein complexes. *Nat. Struct. Biol.* **7**, 220–223
34. Nakanishi, T., Miyazawa, M., Sakakura, M., Terasawa, H., Takahashi, H., and Shimada, I. (2002) Determination of the interface of a large protein complex by transferred cross-saturation measurements. *J. Mol. Biol.* **318**, 245–249
35. Kraulis, P.J. (1991) A program to produce both detailed and schematic plots of protein structures. *J. Appl. Crystallogr.* **24**, 946–950
36. Bacon, D.J. and Anderson, W.F. (1988) A fast algorithm for rendering space-filling molecule pictures. *J. Mol. Graphics* **6**, 219–220
37. Merritt, E.A. and Murphy, M.E. (1994) Raster3D Version 2.0. A program for photorealistic molecular graphics. *Acta Crystallogr. D Biol. Crystallogr.* **50**, 869–873
38. Merritt, E.A. and Bacon, D.J. (1997) Raster3D: Photorealistic Molecular Graphics. *Methods Enzymol.* **277**, 505–524
39. Sali, A. and Blundell, T.L. (1993) Comparative protein modelling by satisfaction of spatial restraints. *J. Mol. Biol.* **234**, 779–815
40. Gouet, P., Courcelle, E., Stuart, D.I., and Metoz, F. (1999) ESPript: analysis of multiple sequence alignments in PostScript. *Bioinformatics* **15**, 305–308